Spectroscopic Observation of Resonant Electric Dipole-Dipole Interactions between Cold Rydberg Atoms

K. Afrousheh, P. Bohlouli-Zanjani, D. Vagale, A. Mugford, M. Fedorov, and J. D. D. Martin
Department of Physics and Institute for Quantum Computing, University of Waterloo, Waterloo, ON, N2L 3G1, Canada
(Received 29 April 2004; published 30 November 2004)

Resonant electric dipole-dipole interactions between cold Rydberg atoms were observed using microwave spectroscopy. Laser-cooled ^{85}Rb atoms in a magneto-optical trap were optically excited to $45d_{5/2}$ Rydberg states using a pulsed laser. A microwave pulse transferred a fraction of these Rydberg atoms to the $46p_{3/2}$ state. A second microwave pulse then drove atoms in the $45d_{5/2}$ state to the $46d_{5/2}$ state, and was used as a probe of interatomic interactions. The spectral width of this two-photon probe transition was found to depend on the presence of the $46p_{3/2}$ atoms, and is due to the resonant electric dipole-dipole interaction between $45d_{5/2}$ and $46p_{3/2}$ Rydberg atoms.

DOI: 10.1103/PhysRevLett.93.233001 PACS numbers: 32.80.Rm, 32.80.Pj, 34.20.Cf

The vast separation of the electron and ion-core in high-n Rydberg atoms is responsible for their large transition dipole moments [1]. These dipole moments dictate the strength of the dipole-dipole interaction between pairs of atoms. Therefore, excitation to Rydberg states allows one to turn on strong interactions between atoms which would otherwise be negligible. This has recently received considerable attention in the context of quantum information processing with cold neutral atoms [2–7]. For example, it has been proposed that a single excited Rydberg atom in a cloud may block further resonant excitation due to the dipole-dipole interaction, a process known as "dipole blockade" [3]. This would allow clouds of cold atoms to store qubits without the addressing of individual atoms and may also be useful for constructing single-atom and single-photon sources [5].

Nonresonant dipole-dipole (van der Waals) interactions between Rydberg atoms were first observed by Raimond *et al.* [8] using spectral line broadening. Recently it has been shown that Rydberg excitation densities in a magneto-optical trap (MOT) are limited by these interactions [9,10]. Dipole-dipole interactions between Rydberg atoms have also been studied in the context of resonant energy transfer [1]. Of particular relevance to this work is the observation of resonant energy transfer between cold Rydberg atoms [11,12], where the Rydberg atoms behave more like an amorphous solid than a gas, and one cannot solely consider binary interactions to explain the transfer process [13,14]. However, use of the resonant dipole-dipole interaction between cold Rydberg atoms to influence radiative transitions, as presented in this work, is an unexplored area.

We excite Rydberg states using a pulsed laser with no stringent demands on linewidth or stability. Dipole-dipole interactions are then introduced and probed using microwave transitions between Rydberg states. This is advantageous since commercial microwave synthesizers are readily tunable, highly stable, and have easily adjustable powers and pulse widths, as compared to lasers. Using this approach we have made the first spectroscopic observation of the *resonant* dipole-dipole interaction between cold Rydberg atoms using radiative transitions.

To observe interactions between atoms that are effectively stationary, we excite Rydberg states of laser-cooled atoms. A standard MOT is used as a source of cold ^{85}Rb atoms. The cooling and trapping light remains on during the experiment and thus a fraction of atoms are in the excited $5p_{3/2}$ state. A Littman-Metcalf, Nd:YAG pumped, nanosecond pulsed dye laser is used to excite these translationally cold $5p_{3/2}$ atoms to the $45d_{5/2}$ state. The total number of Rydberg atoms excited is sensitive to the frequency spectrum of the multimode dye laser, which varies from shot to shot. Since we are interested in density-dependent effects, data is recorded for every laser shot and processed to select laser shots corresponding to specified Rydberg atom densities [15]. The fluctuations may even be considered advantageous, as they allow a range of Rydberg densities to be sampled automatically.

The MOT is formed between two metal plates 3.6 cm apart. These plates contain small holes to let the cooling and trapping lasers through. During laser excitation, an electric field of 5.1 V/cm is applied using these plates, which removes ions formed during laser excitation. This field is switched off with a 0.2 μs fall time approximately 0.1 μs after photoexcitation, and remains less than 0.1 V/cm during application of the microwave pulses (this is verified by observing the Stark shifts of the microwave transitions [16]).

After optical excitation to the $45d_{5/2}$ state, a fraction of the atoms may be transferred to either the $46p_{3/2}$ state or the $45p_{3/2}$ state using a microwave pulse to drive a one-photon transition (the "transfer pulse") (see Fig. 1). The microwave radiation is introduced into the experimental region by horns placed outside the vacuum chamber, directed towards the trapped atom cloud through a large fused silica viewport. To obtain 50 % ($\pm$10%) transfer of Rydberg atoms from the $45d_{5/2}$ to the $46p_{3/2}$ state in 0.6 μs long pulses requires less than 1 mW.

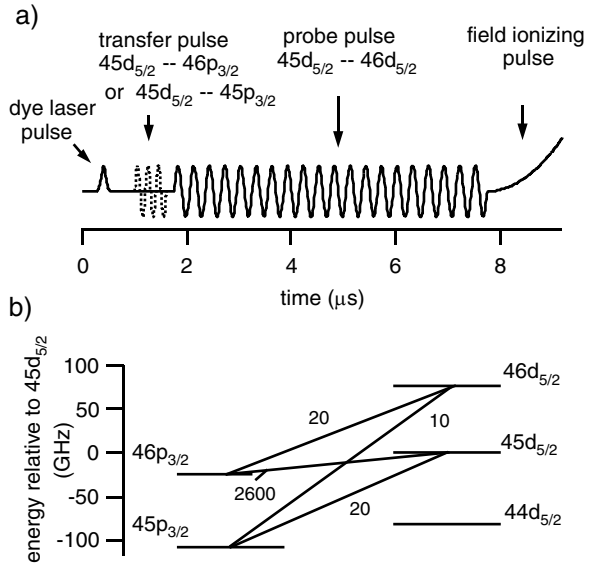

FIG. 1. (a) Timing for experiment and (b) energy levels of relevant states. The spectroscopic data are from Ref. [17]. The matrix elements magnitudes $|\langle n\ell_j|r|n'\ell'_{j'}\rangle|$ are shown between states (in atomic units).

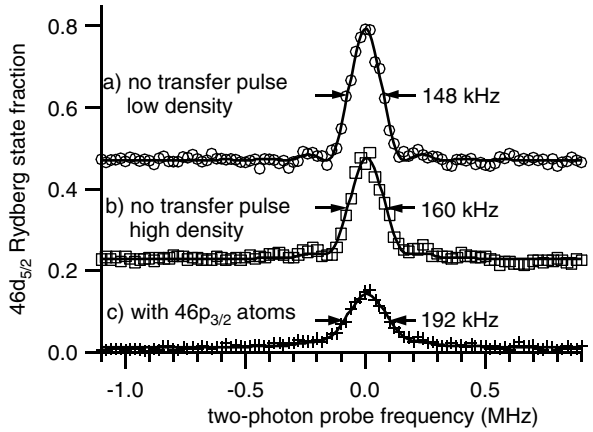

FIG. 2. Observation of the two-photon $45d_{5/2}$–$46d_{5/2}$ microwave transition with (a) (○) all Rydberg atoms initially in the $45d_{5/2}$ state at a density of 2×10^6 cm^{-3}, (b) (□) all Rydberg atoms initially in the $45d_{5/2}$ state at a density of 1×10^7 cm^{-3}, and (c) (+) one-half of the Rydberg atoms initially in the $45d_{5/2}$ state and the other half in the $46p_{3/2}$ state with a total density of 1×10^7 cm^{-3}. Also shown with solid lines are (a) the $\mathrm{sinc}^2(\pi fT)$ line shape ($T = 6$ μs), and (b) and (c) the same line shape convolved with a Lorentzian of variable width to give the best least-squares fits (see text). Spectra are offset vertically for clarity. The probe frequency shown on the horizontal axis is twice the applied frequency, offset by 76.4543 GHz.

To observe dipole-dipole interactions from the line broadening of spectroscopic transitions, it is desirable to minimize other sources of broadening. In particular, the inhomogeneous magnetic fields necessary for operation of the MOT may broaden spectroscopic transitions due to the Zeeman effect. However, as Li *et al.* [17] have demonstrated, two-photon transitions between Rydberg states with the same g_J factors [e.g., $nd_{5/2} - (n+1)d_{5/2}$] show negligible broadening in a MOT. Thus, we use the $45d_{5/2}$–$46d_{5/2}$ two-photon transition as a high resolution, sensitive "probe" of interatomic interactions. This 6 μs probe pulse requires a total power of less than 100 μW and is introduced to the atoms in the same manner as the transfer pulses. The probe frequency is typically scanned between laser shots and the Rydberg state populations are measured after each shot using the selective field ionization (SFI) technique [1]. Absolute, spatially averaged Rydberg densities are obtained from knife-edge measurements of the dye laser beam waist, $5p_{3/2}$ fluorescence imaging, and calibration of the microchannel plate detector. These estimated densities are systematically uncertain by a factor of 2.

Figure 2(a) shows a microwave spectrum of the two-photon probe transition without the application of a transfer pulse. This is well matched by a superimposed $\mathrm{sinc}^2(\pi fT)$ line shape suitable for a square excitation pulse of duration $T = 6$ μs. As expected, inhomogeneous Zeeman broadening makes a negligible contribution to the linewidth [17].

We enhance the interactions between Rydberg atoms by introducing a microwave pulse shortly after photoexcitation, transferring 50% of atoms to the $46p_{3/2}$ state, before application of the two-photon $45d_{5/2}$–$46d_{5/2}$ probe pulse. Unlike the two-photon probe pulse, the one-photon transition is broadened by several MHz due to the inhomogeneous magnetic field [17]. We do not observe any Rabi flopping for this "transfer" transition and consequently do not investigate the possibility of preparing coherent superpositions of these two states. With a total Rydberg density of 10^7 cm^{-3}, converting half of the initially excited $45d_{5/2}$ atoms to the $46p_{3/2}$ state consistently broadens the linewidth of the two-photon $45d_{5/2}$–$46d_{5/2}$ probe transition from 160 ± 5 kHz to 192 ± 5 kHz; see Fig. 2 (all widths in this Letter are full width at half maximum).

As mentioned previously, fluctuations in Rydberg state excitation efficiency may be exploited to accumulate data over a broad range of density conditions. To analyze linewidths quantitatively a $\mathrm{sinc}^2(\pi fT)$ line shape ($T = 6$ μs) is convolved by a Lorentzian with a variable width $\delta\nu$ adjusted for the best least-squares fit to individual spectra. The Lorentzian form is supported by a theoretical model (*vide infra*). Figure 3 shows $\delta\nu$ both with and without introduction of the $46p_{3/2}$ atoms, as a function of average Rydberg density. With decreasing density $\delta\nu$ approaches zero, suggesting the influence of interatomic interactions, which inevitably weaken at the large average separations corresponding to low densities.

The difference in linewidths with and without the $46p_{3/2}$ atoms can be attributed to resonant electric

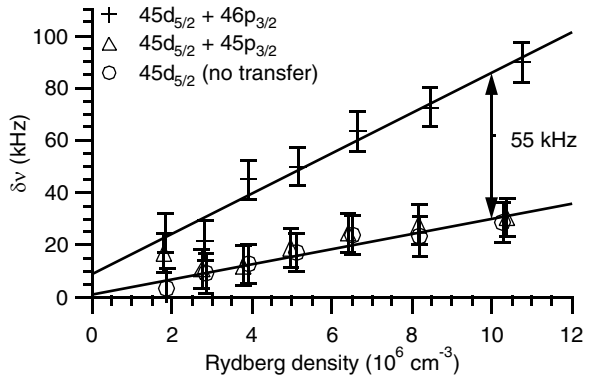

FIG. 3. Broadening of the $45d_{5/2}$–$46d_{5/2}$ probe transition as a function of average Rydberg density with and without the transfer pulses (see text for definition of $\delta\nu$).

dipole-dipole interactions. To obtain estimates of the line broadening we consider interactions between pairs of atoms (A and B) due to the electric dipole-dipole interaction operator:

$$\hat{V}_{dd} = \frac{\vec{\mu}_{\rm A}\cdot\vec{\mu}_{\rm B} - 3(\vec{\mu}_{\rm A}\cdot\vec{n})(\vec{\mu}_{\rm B}\cdot\vec{n})}{R_{\rm AB}^3}, \qquad (1)$$

where $\vec{\mu}_{\rm A}$ and $\vec{\mu}_{\rm B}$ are the electric dipole matrix element operators evaluated on each atom, $\vec{n}$ is the unit vector pointing between the atoms, and $R_{\rm AB}$ is the separation of the two atoms. This perturbation may split the otherwise energy degenerate states $|1\rangle = |45d_{5/2}m_{j,{\rm A}1}\rangle_{\rm A}|46p_{3/2}m_{j,{\rm B}1}\rangle_{\rm B}$ and $|2\rangle = |46p_{3/2}m_{j,{\rm A}2}\rangle_{\rm A} \times |45d_{5/2}m_{j,{\rm B}2}\rangle_{\rm B}$, and with a 50% mixture of $45d_{5/2}$ and $46p_{3/2}$ atoms we can obtain a very rough idea of the magnitude of the energy splittings from $\Delta\nu_{dd} \approx \mu^2/R^3$, where $\mu = |\langle 45d_{5/2,1/2}|\mu_z|46p_{3/2,1/2}\rangle| \approx 0.49|\langle 45d_{5/2}| \times r|46p_{3/2}\rangle|$, $R = (4\pi n_{46p}/3)^{-1/3}$, and n_{46p} is the $46p_{3/2}$ number density. The radial matrix element is evaluated by numerical integration of the Rydberg electron wave functions [see Fig. 1(b)] [18]. The $45d_{5/2}$ and $46p_{3/2}$ states are strongly dipole coupled, whereas the $46d_{5/2}$ and $46p_{3/2}$ states are not. Therefore, only the initial state of the two-photon probe transition is split by the resonant dipole-dipole interaction with $46p_{3/2}$ atoms. A density of $n_{46p} = 5\times10^6$ cm^{-3} gives $\Delta\nu_{dd} = 33$ KHz, the same order of magnitude as the observed broadening (see Fig. 3).

The dipole coupling between the $45d_{5/2}$ and $45p_{3/2}$ states is much smaller than that between the $45d_{5/2}$ and $46p_{3/2}$ states [see Fig. 1(b)]. This suggests the following test. Instead of transferring 50% of the atoms to the $46p_{3/2}$ state, we transfer 50% of atoms to the $45p_{3/2}$ state, and study the broadening of the probe transition with increasing Rydberg atom density. Based on the much smaller dipole matrix element, it is expected that introducing the $45p_{3/2}$ atoms will have little influence on the linewidth of the probe transition. Figure 3 shows that the introduction of the $45p_{3/2}$ atoms gives linewidths which are experimentally indistinguishable from the 100% $45d_{5/2}$ case.

Now we consider a calculation of the linewidths which accounts for the orientations of the dipole and $\vec{n}$ operators and the distribution in interacting atom separations, which were neglected in the simple estimate presented above. With no magnetic field, there is a large energy degeneracy corresponding to the different possible magnetic sublevels for the two atoms (A and B) (without $\hat{V}_{dd}$). However, in the MOT the average Zeeman shifts are relatively large ($\approx$1 MHz) compared to the influence of $\hat{V}_{dd}$(<100 kHz). Therefore only those states that are exactly degenerate are strongly coupled ($m_{j,{\rm A}1} = m_{j,{\rm B}2}$ and $m_{j,{\rm B}1} = m_{j,{\rm A}2}$). In the absence of detailed information about the magnetic sublevel populations, two extremes are considered: (a) atoms are randomly distributed over all possible magnetic sublevels, and (b) all atoms are in $m_j = 1/2$. In the first case the effective interaction is diminished, since there will be pairs of atoms which will not interact at all (e.g., $m_{j,{\rm A}1} = 5/2$, $m_{j,{\rm B}1} = -3/2$). To simulate the line shape, in particular, the randomness associated with $R_{\rm AB}$ and $\vec{n}$, we consider a $45d_{5/2}$ atom at the center of a sphere containing a number of randomly placed $46p_{3/2}$ atoms. The matrix elements $\langle 1|\hat{V}_{dd}|2\rangle$ are computed using the $45d_{5/2}$ atom and each $46p_{3/2}$ within the sphere, using the magnetic sublevel distribution scenarios discussed above. The matrix element with the largest magnitude is selected $V_{\rm max}$ (a binary "strongest interacting" neighbor approximation). This splits the $45d_{5/2}$–$46d_{5/2}$ transition into a doublet $\pm V_{\rm max}$ (the energy eigenvalues of our simplified two-state system). This process was repeated numerous times, and the resulting splittings histogramed to obtain line shapes, which converged as the size of the sphere and number of particles increased (we maintained a constant average density). These have sharp dips in their centers, but Lorentzian wings (the dips are much sharper than the transform-limited linewidth at the densities studied here).

The simulated line shapes were convolved with a $\mathrm{sinc}^2(\pi fT)$ line shape ($T = 6$ μs) and fitted in the same manner as the experimental data (using the $\mathrm{sinc}^2(\pi fT)$ line shape convolved with a Lorentzian of adjustable width $\delta\nu_{dd}$). With $n_{46p} = 5\times10^6$ cm^{-3} (corresponding to 10^7 cm^{-3} total density) we get $\delta\nu_{dd} = 18$ kHz and $\delta\nu_{dd} = 63$ kHz for cases (a) and (b) discussed above. As Fig. 3 shows, the experimentally observed increase in $\delta\nu$ at this density is 55 ± 5 kHz, in reasonable agreement with the calculations. In making this comparison, it is assumed that the mechanism producing the density-dependent $\delta\nu$ observed with no $46p_{3/2}$ atoms, is also present with the introduction of $46p_{3/2}$ atoms, and its contribution is additive, which should be reconsidered

in a more precise study. Our Rydberg density estimate is uncertain by a factor of 2, and thus an improvement in this would be desirable for testing the limitations of this theoretical estimate (e.g., binary approximation, magnetic sublevel distributions, constant line strengths).

These estimates of line broadening have not accounted for motion of the Rydberg atoms. Consider two atoms separated by 35 μm, heading towards each other with a relative speed of 0.4 m/s (typical of a density of 5×10^6 cm^{-3} and a temperature of 300 μK). Over the 8 μs of the experiment their relative distance will change by only 9%. The acceleration of $45d_{5/2}$ and $46p_{3/2}$ atoms towards (or away from) one another, due to the gradient of V_{dd}, should also be considered [19]. The force $|\vec{F}| = |\vec{\nabla} V_{dd}| \approx 3\mu^2/R^4$ produces a relative acceleration of 25 m/s^2 at a separation of 35 μm. Over 8 μs, this acceleration does not change the separation appreciably, the assumption of interactions between stationary atoms is reasonable. In this regard, our translationally cold Rydberg atoms are analogous to amorphous solid-state systems [20]. However, since the force due to $\hat{V}_{dd}$ has a strong R dependence, and the atoms do have some thermal motion, there will be a (small) fraction of close atom pairs for which movement should not be neglected, especially at higher densities than those considered here [19].

With no deliberate introduction of $46p_{3/2}$ atoms it is observed that linewidth broadens linearly with Rydberg density (see Fig. 3). Nonresonant dipole-dipole interactions are too weak to explain this, and would not show a linear density dependence. We are at densities well below the regime of spontaneous plasma formation [15,21] (we observe an ion signal that is 3% of the Rydberg signal at 10^7 cm^{-3}, too low to give appreciable broadening due to the Stark effect from inhomogeneous electric fields). Trapped electron collisions [22] could broaden the transition lines. Again, we do not expect these to give a linear density dependence. The arguments of the previous paragraph rule out collisions between cold Rydberg atoms, but collisions with hot Rydberg atoms from the background vapor may be important [15]. At a density of 10^7 cm^{-3} we observe significant ($\approx$10%) redistribution of the initially excited Rydberg state population into higher angular momentum states ($l > 2$), and this redistribution scales linearly with Rydberg density, like the observed broadening. The observed redistribution rate diminishes in time following photoexcitation, as expected for collisions with hot atoms (which diffuse from the excitation region). Thus we believe that either collisions with the hot Rydberg atoms, or the products of these collisions, are responsible for the broadening, and are currently investigating the specific mechanism.

In summary, we have observed line broadening in the microwave spectra of Rydberg atoms due to resonant electric dipole-dipole interactions, using a combination of laser and microwave excitation sources. This is a general approach to the study of cold Rydberg atom interactions. For example, a combination of crossed optical excitation beams (to achieve a small excitation volume) together with microwave transitions could allow observation of the dipole blockade phenomena [3].

This work was supported by NSERC, CFI, and OIT. We thank J. Keller, J. Carter, P. Haghnegahdar, and A. Colclough for assistance.

[1] T. F. Gallagher, *Rydberg Atoms* (Cambridge University Press, Cambridge, England, 1994).
[2] D. Jaksch *et al.*, Phys. Rev. Lett. **85**, 2208 (2000).
[3] M. D. Lukin *et al.*, Phys. Rev. Lett. **87**, 037901 (2001).
[4] I. E. Protsenko, G. Reymond, N. Schlosser, and P. Grangier, Phys. Rev. A **65**, 052301 (2002).
[5] M. Saffman and T. G. Walker, Phys. Rev. A **66**, 065403 (2002).
[6] M. S. Safronova, C. J. Williams, and C. W. Clark, Phys. Rev. A **67**, 040303 (2003).
[7] I. I. Ryabtsev, D. B. Tretyakov, and I. I. Beterov, quant-ph/0402006.
[8] J. M. Raimond, G. Vitrant, and S. Haroche, J. Phys. B **14**, L655 (1981).
[9] D. Tong *et al.*, Phys. Rev. Lett. **93**, 063001 (2004).
[10] K. Singer, M. Reetz-Lamour, T. Amthor, L. G. Marcassa, and M. Weidemüller, Phys. Rev. Lett. **93**, 163001 (2004).
[11] W. R. Anderson, J. R. Veale, and T. F. Gallagher, Phys. Rev. Lett. **80**, 249 (1998).
[12] I. Mourachko *et al.*, Phys. Rev. Lett. **80**, 253 (1998).
[13] W. R. Anderson, M. P. Robinson, J. D. D. Martin, and T. F. Gallagher, Phys. Rev. A **65**, 063404 (2002).
[14] I. Mourachko, W. Li, and T. F. Gallagher, Phys. Rev. A **70**, 031401 (2004).
[15] M. P. Robinson, B. L. Tolra, M. W. Noel, T. F. Gallagher, and P. Pillet, Phys. Rev. Lett. **85**, 4466 (2000).
[16] A. Osterwalder and F. Merkt, Phys. Rev. Lett. **82**, 1831 (1999).
[17] W. Li, I. Mourachko, M. W. Noel, and T. F. Gallagher, Phys. Rev. A **67**, 052502 (2003).
[18] M. L. Zimmerman, M. G. Littman, M. M. Kash, and D. Kleppner, Phys. Rev. A **20**, 2251 (1979).
[19] A. Fioretti, D. Comparat, C. Drag, T. F. Gallagher, and P. Pillet, Phys. Rev. Lett. **82**, 1839 (1999).
[20] R. M. Macfarlane and R. M. Shelby, Opt. Commun. **39**, 169 (1981).
[21] T. C. Killian *et al.*, Phys. Rev. Lett. **83**, 4776 (1999).
[22] S. K. Dutta, D. Feldbaum, A. Walz-Flannigan, J. R. Guest, and G. Raithel, Phys. Rev. Lett. **86**, 3993 (2001).